

Photolysis frequency of NO₂: Measurement and modeling during the International Photolysis Frequency Measurement and Modeling Intercomparison (IPMMI)

R. E. Shetter,¹ W. Junkermann,² W. H. Swartz,³ G. J. Frost,⁴ J. H. Crawford,⁵ B. L. Lefer,¹ J. D. Barrick,⁵ S. R. Hall,¹ A. Hofzumahaus,⁶ A. Bais,⁷ J. G. Calvert,¹ C. A. Cantrell,¹ S. Madronich,¹ M. Müller,⁶ A. Kraus,⁶ P. S. Monks,⁸ G. D. Edwards,⁸ R. McKenzie,⁹ P. Johnston,⁹ R. Schmitt,¹⁰ E. Griffioen,¹¹ M. Krol,¹² A. Kylling,¹³ R. R. Dickerson,¹⁴ S. A. Lloyd,³ T. Martin,^{2,15} B. Gardiner,¹⁶ B. Mayer,^{2,17} G. Pfister,¹ E. P. Röth,¹⁸ P. Koepke,¹⁹ A. Ruggaber,¹⁹ H. Schwander,¹⁹ and M. van Weele²⁰

Received 10 September 2002; revised 23 December 2002; accepted 6 February 2003; published 3 June 2003.

[1] The photolysis frequency of NO₂, $j(\text{NO}_2)$, was determined by various instrumental techniques and calculated using a number of radiative transfer models for 4 days in June 1998 at the International Photolysis Frequency Measurement and Modeling Intercomparison (IPMMI) in Boulder, Colorado. Experimental techniques included filter radiometry, spectroradiometry, and chemical actinometry. Eight research groups participated using 14 different instruments to determine $j(\text{NO}_2)$. The blind intercomparison experimental results were submitted to the independent experimental referee and have been compared. Also submitted to the modeling referee were the results of NO₂ photolysis frequency calculations for the same time period made by 13 groups who used 15 different radiative transfer models. These model results have been compared with each other and also with the experimental results. The model calculation of clear-sky $j(\text{NO}_2)$ values can yield accurate results, but the accuracy depends heavily on the accuracy of the molecular parameters used in these calculations. The instrumental measurements of $j(\text{NO}_2)$ agree within the uncertainty of the individual instruments and indicate the stated uncertainties in the instruments or the uncertainties of the molecular parameters may be overestimated. This agreement improves somewhat with the use of more recent NO₂ cross-section data reported in the literature. *INDEX TERMS*: 0360 Atmospheric Composition and Structure: Transmission and scattering of radiation; 0365 Atmospheric Composition and Structure: Troposphere—composition and chemistry; 0394 Atmospheric Composition and Structure: Instruments and techniques; *KEYWORDS*: photolysis, NO₂ (nitrogen dioxide), radiative transfer, intercomparison

Citation: Shetter, R. E., et al., Photolysis frequency of NO₂: Measurement and modeling during the International Photolysis Frequency Measurement and Modeling Intercomparison (IPMMI), *J. Geophys. Res.*, 108(D16), 8544, doi:10.1029/2002JD002932, 2003.

¹Atmospheric Chemistry Division, National Center for Atmospheric Research, Boulder, Colorado, USA.

²Institut fuer Meteorologie und Klimaforschung, Forschungszentrum Karlsruhe GmbH, Garmisch-Partenkirchen, Germany.

³Applied Physics Laboratory, Johns Hopkins University, Laurel, Maryland, USA.

⁴Cooperative Institute for Research in Environmental Sciences, University of Colorado, Boulder, Colorado, USA.

⁵NASA Langley Research Center, Hampton, Virginia, USA.

⁶Institut fuer Chemie und Dynamik der Geosphäre Institut II: Troposphäre, Forschungszentrum Jülich GmbH, Jülich, Germany.

⁷Laboratory of Atmospheric Physics, Aristotle University of Thessaloniki, Thessaloniki, Greece.

⁸University of Leicester, Leicester, UK.

⁹National Institute of Water and Atmospheric Research, Lauder, New Zealand.

¹⁰Meteorologie Consult GmbH, Glashütten, Germany.

¹¹Meteorological Service of Canada, Toronto, Ontario, Canada.

¹²Institute for Marine and Atmospheric Research, Utrecht, Netherlands.

¹³Norwegian Institute for Air Research, Kjeller, Norway.

¹⁴Department of Meteorology, University of Maryland, College Park, Maryland, USA.

¹⁵Also at Institute for Geophysics, Astrophysics and Meteorology (IGAM), Karl-Franzens University of Graz, Graz, Austria.

¹⁶British Antarctic Survey, Cambridge, UK.

¹⁷Now at Institut fuer Physik der Atmosphaere, Deutsches Zentrum fuer Luft und Raumfahrt, Wessling, Germany.

¹⁸Institut fuer Chemie und Dynamik der Geosphäre Institut I: Stratosphäre, Forschungszentrum Juelich GmbH, Juelich, Germany.

¹⁹Meteorologisches Institut, Universität München, Munich, Germany.

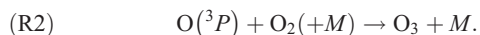
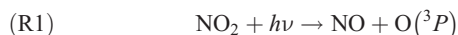
²⁰Royal Netherlands Meteorological Institute, DeBilt, Netherlands.

1. Introduction

[2] Ultraviolet and visible solar radiation drives much of the chemistry in the troposphere by dissociating molecules into reactive species that enter atmospheric chemical cycles. Measurements of atmospheric photolysis frequencies (photolysis rate coefficients, or j values) are therefore important in the study of atmospheric chemical processes. Current atmospheric chemistry studies require the accurate determination of j values in order to understand NO_x and HO_x cycling and reactive radical production. The photolysis frequency of NO₂ is the first-order rate coefficient of the dissociation process. Photolysis frequencies can be calculated from

$$j(\text{NO}_2) = \int F(\lambda)\sigma(\lambda, T, P)\phi(\lambda, T, P)d\lambda, \quad (1)$$

where $j(\text{NO}_2)$ is the photolysis frequency of the dissociation of NO₂ to NO and O(³P); F is the in situ solar actinic flux; σ is the absorption cross section of NO₂ as a function of wavelength (λ), temperature (T), and pressure (P); and ϕ is the quantum yield of the photodissociation products as a function of λ , T , and P . The j value of NO₂ determines the partitioning of NO_x (the photostationary state of NO₂, NO, and O₃), as well as the photochemical production of O₃ by reactions (R1) and (R2)



[3] The solar actinic flux is the radiation available to a molecule from all directions for initiation of a photodissociation process [Madronich, 1987]. Measurements of the total actinic flux as a function of wavelength combined with molecular parameters (absorption cross sections and quantum yields as a function of pressure and temperature from laboratory measurements) allow one to calculate photolysis frequencies with equation (1).

[4] Measurements of the total actinic flux include contributions from the direct solar beam, scattered and reflected radiation from clouds, aerosols, molecules, and the Earth's surface. Optical collection of the direct, scattered, and reflected radiation for measurement is difficult because of the changing angular distribution of the radiation. Past $j(\text{NO}_2)$ determinations have been performed using three principal methods that have been reported in the literature since the early 1970s, namely, chemical actinometry, filter radiometry, and spectroradiometry.

[5] Chemical actinometers have been used to determine photolysis frequencies of NO₂ [Jackson *et al.*, 1975; Harvey *et al.*, 1977; Bahe, 1980; Dickerson *et al.*, 1982; Parrish *et al.*, 1983; Madronich *et al.*, 1984, 1985; Shetter *et al.*, 1992; Schultz *et al.*, 1995; Lantz *et al.*, 1996; Kraus *et al.*, 2000]. These instruments expose the NO₂ to solar radiation and measure a product of the photodissociation process to determine the atmospheric photolysis frequency of NO₂. Therefore actinometry does not depend on molecular parameters but depends on a chemical calibration of a

reactant or product or calibration of pressure change. Most actinometers employ a flow of gas through a quartz tube, but static tubes or bulbs have also been used. The tube geometry provides a reasonable 2π sr field of view assuming tube length to diameter ratios >10 and proper field of view setup. Sampling frequency of chemical actinometers varies from 2 s to longer than 60 min.

[6] Filter radiometers have also been employed to determine photolysis frequencies of NO₂ [Junkermann *et al.*, 1989; Brauers and Hofzumahaus, 1992; Volz-Thomas *et al.*, 1996]. These radiometers use band-pass filters designed to simulate the absorption cross section-quantum yield product of the molecule of interest and are usually calibrated against a chemical actinometer. The optical collection schemes of radiometers vary from flat plate (cosine response) devices to hemispherical actinic flux collectors as described by Junkermann *et al.* [1989]. Flat plate collectors require cosine correction as a function of zenith angle that can become very difficult in complex atmospheric environments involving aerosols, clouds, and changing albedos. These problems are not encountered with actinic flux collector filter radiometers. Response speed and the small instrument size of filter radiometers make them reasonable choices for field use, but a different radiometer is required for each photolysis frequency determined, and the calibration of the filter radiometers exhibits weak dependences on solar zenith angle, temperature, and cloudiness [Volz-Thomas *et al.*, 1996].

[7] Spectroradiometer measurements of NO₂ photolysis frequencies have been reported recently by Kraus *et al.* [1998a], Kraus and Hofzumahaus [1998], Hofzumahaus *et al.* [1999], Shetter and Müller [1999], Kraus *et al.* [2000], Pätz *et al.* [2000], Lefer *et al.* [2001a, 2001b], and Shetter *et al.* [2003]. Actinic flux spectroradiometers determine solar actinic flux as a function of wavelength. Atmospheric photolysis frequencies can be calculated for any molecule whose absorption spectrum falls in the wavelength range measured, using the molecular cross-section and quantum yield data as a function of temperature and pressure for the photolysis process of interest. The calculated photolysis frequencies are subject to the uncertainties associated with the cross sections and quantum yields but could be recalculated from the actinic flux data if the molecular data are redetermined at a later date.

2. Experimental Procedure

[8] During the International Photolysis Frequency Measurement and Modeling Intercomparison (IPMMI) campaign, 14 different instruments were used by eight different groups to measure $j(\text{NO}_2)$: two chemical actinometers, five spectroradiometers, and seven filter radiometers. A listing of the instruments, the research groups participating, and the identification abbreviations is given in Table 1. While brief instrument descriptions are included below, more complete descriptions of the IPMMI $j(\text{NO}_2)$ instruments and their error analyses can be found in the IPMMI overview paper [Cantrell *et al.*, 2003].

2.1. The $j(\text{NO}_2)$ Chemical Actinometers

[9] Two different chemical actinometer systems used in the measurements of $j(\text{NO}_2)$ were deployed by the National

Table 1. Listing of Participating Instruments and Institutions, International Photolysis Frequency Measurement and Modeling Intercomparison (IPMMI) Instrument Identification, and Quantity Measured

Institution	IPMMI Identification (ID)	Quantity Measured
<i>Chemical Actinometers</i>		
National Center for Atmospheric Research (NCAR) Atmospheric Radiation Investigations and Measurements (ARIM) group	NCAR	$j(\text{NO}_2)$
University of Maryland (UMD)	UMD	$j(\text{NO}_2)$
<i>Spectroradiometers</i>		
Forschungszentrum Jülich	FZJ	actinic flux
Meteorologie Consult GmbH	MET1	actinic flux
National Center for Atmospheric Research ARIM	NCAR	actinic flux
University of Leicester	ULI	actinic flux
National Institute of Water and Atmospheric Research	NIWA	irradiance
<i>Filter Radiometers</i>		
Forschungszentrum Jülich	FZJ	broadband $j(\text{NO}_2)$
Fraunhofer Institut Atmosphärische Umweltforschung	IFU	broadband $j(\text{NO}_2)$
Meteorologie Consult GmbH	MET1	broadband $j(\text{NO}_2)$
Meteorologie Consult GmbH	MET2	broadband $j(\text{NO}_2)$
NASA Langley Research Center	NAL1	broadband $j(\text{NO}_2)$
NASA Langley Research Center	NAL2	broadband $j(\text{NO}_2)$
University of Leicester	ULI	broadband $j(\text{NO}_2)$

Center for Atmospheric Research (NCAR) and University of Maryland (UMD) groups, respectively. In both systems, NO₂ flowing in an O₂-rich mixture is photodissociated by sunlight (reaction (R1)), the O(³P) atom reacts largely to form ozone (reaction (R2)), and the resulting NO product is a measure of the extent of NO₂ photolysis.

2.1.1. National Center for Atmospheric Research

[10] The NCAR $j(\text{NO}_2)$ chemical actinometer deployed for the IPMMI campaign is very similar to the instrument used in the Mauna Loa Observatory Photochemistry Experiment (MLOPEX) and is described by *Shetter et al.* [1992] and *Lantz et al.* [1996]. The primary instrumental difference from the MLOPEX instrument was that a high-pressure cylinder mixture of NO₂ in N₂ was used as the NO₂ source instead of a permeation oven. The instrument consisted of an NO₂ flow delivery system, a quartz photolysis cell for exposure to sunlight, an NO chemiluminescence detector, an NO calibration system, and a data acquisition computer.

[11] The design of the actinometer incorporated a 500 standard cubic centimeter per minute at standard temperature and pressure (cm³ min⁻¹ STP) flow of ~2 ppm NO₂ in ultrahigh-purity O₂ through the photolysis cell (1.000 cm in diameter and 50 cm in length) at reduced pressure (~50 torr) that was exposed to sunlight for ~0.3 s. The NO produced from photolysis was determined by a standard NO chemiluminescence detector, similar to the one used by *Ridley and Howlett* [1974] to measure ambient NO levels. The instrument was calibrated every 1–2 hours by first determining the background NO signal by occluding all ambient light from the photolysis cell with a cylindrical shutter and then determining the instrument response to the addition of 5 cm³ min⁻¹ STP of a NO standard to the sample flow. The instrument backgrounds and NO sensitivities were recorded every hour, and linear interpolations were performed on the data in the final data analysis. The mass flow controllers and NO and NO₂ cylinder concentrations were calibrated directly before and after the IPMMI

program. Minor corrections (<0.2%) were made to correct the measured amount of NO resulting from side reactions forming and destroying NO (e.g., NO + O₃ → NO₂ + O₂, O(³P) + NO₂ → O₂ + NO.)

2.1.2. University of Maryland

[12] The UMD chemical actinometer for $j(\text{NO}_2)$ used during IPMMI was derived from an instrument first designed and fabricated by *Kelley et al.* [1995] (versions thereof have been used previously for measuring $j(\text{NO}_2)$) [*Dickerson et al.*, 1997; *Rhoads et al.*, 1997]. NO₂ was generated by a permeation tube and was diluted to a nominal 4900 ppbv mixing ratio in zero air. The NO₂-air mixture at ambient pressure is exposed to downwelling sunlight (2π sr) in a quartz tube (8.00 mm ID × 179.9 mm exposed length) mounted 4 mm above a flat black plate. NO thus produced by NO₂ photolysis is measured by a modified chemiluminescence NO_x analyzer, which was calibrated immediately before, once during, and after the campaign. Background NO measurements were made twice per hour. The determination of $j(\text{NO}_2)$ is then made directly from the NO and NO₂ concentrations and solar exposure time (0.7 s), with side reaction corrections of <2%.

2.2. Spectroradiometers

[13] Four spectroradiometers were used to measure the downwelling actinic flux, and one spectroradiometer measured the downwelling solar irradiance. Each actinic flux spectroradiometer (NCAR, Forschungszentrum Jülich (FZJ), Meteorologie Consult GmbH (MET1), and University of Leicester (ULI)) independently measured downwelling actinic flux through tower-mounted (~5 m) 2π sr light collection optics, while the National Institute of Water and Atmospheric Research (NIWA) irradiance instrument used a flat plate diffuser with a cosine response to measure the irradiance incident on a horizontal surface at the ground. Three of the systems (NCAR, FZJ, and NIWA) were of the scanning double monochromator type, serially measuring

the wavelengths with each step of a monochromator. The ULI and MET1 instruments employed a diode array single monochromator to measure the actinic flux over the full wavelength range simultaneously. The photolysis frequency data calculated from the actinic flux spectroradiometers are dependent on the NO₂ cross-section and quantum yield data used in the actinic flux to photolysis frequency calculation. In an attempt to assess the current NO₂ cross-section data, investigators reported photolysis frequencies calculated using the *DeMore et al.* [1997] and *Harder et al.* [1997] literature values. The instruments are described briefly in sections 2.2.1–2.2.5.

2.2.1. Forschungszentrum Jülich

[14] The actinic flux spectroradiometer of Forschungszentrum Jülich has been described in detail by *Hofzumahaus et al.* [1999]. During IPMMI, the FZJ spectroradiometer consisted of a 2π sr actinic flux entrance optic (Meteorologie Consult GmbH (METCON)/FZJ), a scanning double monochromator (Bentham DTM 300), a 10-m quartz fiber optic bundle (Gigahertz Optik GmbH), a photoelectric detection system (EMI 9250 photomultiplier), and a computer for data acquisition and system control. Spectra from 280 to 420 nm were typically scanned every 80 s (68 s to scan each spectrum), with a step size of 1.0 nm and a spectral band pass of 1.1 nm full width at half maximum (FWHM). Absolute spectral calibrations were performed with a Physikalisch-Technischen Bundesanstalt traceable irradiance standard (FEL 1000-W quartz lamp, Gigahertz Optik GmbH) on the field site on 14, 17, and 20 June. Additional field calibrations were performed on each day of the campaign. Wavelength calibrations of the monochromator were performed using emission lines of a mercury lamp and by examination of the Fraunhofer structure in the solar spectrum. The FZJ spectroradiometer was previously deployed at ground stations in Germany during the Photo-Oxidant Formation by Plant Emitted Compounds and OH Radicals in North-Eastern Germany (1994) [*Brauers et al.*, 1998], JNO₂ Comparison 1997 (JCOM97) (1997) [*Kraus et al.*, 2000], and BERLIner Ozone experiment (BERLIOZ) (1998) [*Platt et al.*, 2002], on the German ship Polarstern during the Air Chemistry and Lidar Studies above the Atlantic Ocean (1996) [*Burkert et al.*, 2001], and on an aircraft during ATOP (1996).

2.2.2. Meteorologie Consult GmbH

[15] Meteorologie Consult GmbH, Glashütten (METCON), deployed a commercially available spectroradiometer for IPMMI. The instrument consisted of a 2π sr actinic flux entrance optic (METCON), a single monochromator (Carl Zeiss), a 512-pixel diode array detection system (Carl Zeiss), and a computer for data acquisition. The diode array measured wavelengths from 285 to 450 nm in consecutive 0.5-, 1-, 3-, and 5-s integration times with a spectral band pass of ~ 2.2 nm FWHM. A spectral calibration was performed before IPMMI using the 1000-W National Institute of Standards and Technology (NIST) traceable quartz tungsten halogen (QTH) lamps in the NCAR laboratory calibration facility.

2.2.3. National Center for Atmospheric Research

[16] The NCAR Scanning Actinic Flux Spectroradiometer (SAFS) has been described in detail by *Shetter and Müller* [1999]. As installed during IPMMI, the SAFS instrument consisted of a 2π sr actinic flux entrance optic

(METCON/NCAR), a 12-m custom fiber optic bundle with high UV throughput (CeramOptec), a double monochromator (CVI Digikrom CM 112), a photomultiplier tube (Electron Tubes, Ltd.), a custom designed four-stage current-to-voltage amplifier, and a computer for fully automated data acquisition and system control. Spectra from 280 to 420 nm were scanned every 15 s (10 s to scan each spectrum) by stepping in 1.0-nm increments from 280 to 330 nm and in 2.0-nm increments from 330 to 420 nm. The spectral band pass (FWHM) was 1.0 nm with a triangular slit function. Absolute spectral calibrations were performed with a NIST traceable irradiance standard (1000-W QTH lamp, Oriel Instruments, 63350) in the NCAR laboratory before and after the intercomparison. Field calibrations were performed with 250-W secondary QTH lamps for several weeks before, during (17 June), and after the project to assess the relative stability of the instrument sensitivity. Wavelength calibrations of the monochromator were performed in conjunction with each spectral calibration using the emission lines from a mercury lamp. SAFS instruments have been previously deployed on aircraft during NASA Global Tropospheric Experiment (GTE) Pacific Exploratory Mission (PEM)-Tropics A mission (1996), NASA AEAP SONEX mission (1997), National Oceanic and Atmospheric Administration (NOAA) Southern Oxidants Study (SOS) Nashville study (1999), NASA GTE PEM-Tropics B mission (1999), NASA Upper Atmosphere Research Program SAGE III Ozone Loss and Validation Experiment mission (2000), National Science Foundation (NSF) ACD Tropospheric Ozone Production About the Spring Equinox mission (2000), and NASA Transport and Atmospheric Chemistry Near the Equator—Pacific (TRACE-P) mission (2001) and at ground sites for the SOS Nashville field study in 1999, Program for Research on Oxidants: Photochemistry, Emissions, and Transport field studies in 2000 and 2001, and NSF Polar Programs Investigation of Sulfur Chemistry in the Antarctic Troposphere 1998 and 2000 field studies.

2.2.4. University of Leicester

[17] The University of Leicester deployed a commercially available diode array spectroradiometer (METCON) for the intercomparison. The instrument consisted of a 2π sr actinic flux entrance optic (METCON), a single monochromator (Carl Zeiss), a 512-pixel diode array detection system (Carl Zeiss), and a computer for data acquisition. The diode array measured wavelengths from 285 to 450 nm in consecutive 0.5-, 1-, 3-, and 5-s integration times with a spectral band pass of ~ 2.2 nm FWHM. A spectral calibration was performed during IPMMI using the 1000-W NIST traceable QTH lamps in the NCAR laboratory calibration facility. After the intercomparison the instrument was again calibrated using a 200-W NIST traceable QTH lamp (Oriel) at the University of Leicester. Wavelength calibrations of the diode array were performed using the emission lines from mercury and sodium lamps. A full description of the ULI instrument is given by *Edwards and Monks* [2003].

2.2.5. New Zealand National Institute of Water and Atmospheric Research

[18] The NIWA spectroradiometer employed a flat plate diffuser with a cosine response to measure the irradiance incident on a horizontal surface. The instrument has been

described in detail by *McKenzie et al.* [1992, 2002]. Recent modifications include replacement of the original diffuser with an in-house designed diffuser coupled to the instrument via a fiber optic bundle, resulting in a greatly improved cosine response. As installed during IPMMI, the NIWA instrument consisted of a PTFE diffuser, a double monochromator (JYDH10), a photomultiplier tube (Electron Tubes, Ltd., Model 9804 QA), and an automated data acquisition and system control computer. Spectra from 290 to 450 nm were scanned every 190 s with a repetition rate of 5 min by stepping in 0.2-nm increments. The spectral band pass (FWHM) was 1.3 nm. An absolute spectral calibration was performed with a NIST traceable irradiance standard (1000-W QTH lamp) using the NOAA field calibration facility described by *Early et al.* [1998] during the inter-comparison. For this instrument the measured cosine weighted irradiances were reported as “pseudoactinic fluxes” rather than “actinic fluxes”. The pseudoactinic fluxes were then integrated with the NO₂ molecular parameters to calculate a “pseudo”- $j(\text{NO}_2)$ [see *McKenzie et al.*, 2002].

2.3. The $j(\text{NO}_2)$ Filter Radiometers

[19] All of the participating $j(\text{NO}_2)$ filter radiometers were commercially available instruments manufactured by METCON. The METCON $j(\text{NO}_2)$ filter radiometer is based on the concept of *Junkermann et al.* [1989] and includes technical modifications of the inlet optic and optical filter combination as described by *Volz-Thomas et al.* [1996]. The entrance optic of the radiometer consists of diffusively transmitting quartz domes and has a nearly uniform angular response to radiation incident from the upper hemisphere (2π sr). The collected radiation is optically filtered by a glass filter combination (2-mm UG3, 1-mm UG5, Schott GmbH) and is detected by a vacuum photodiode having a Cs-Sb photocathode. A single-stage current-to-voltage amplifier converts the photocurrent into a voltage signal. The signal of the filter radiometer depends on the broadband integrated actinic flux between 310 and 420 nm and is nearly proportional to the NO₂ photolysis frequency.

2.3.1. Meteorologie Consult GmbH

[20] The METCON filter radiometer is described in section 2.3. The METCON factory calibration can be traced back to a yearly calibration with a chemical actinometer measuring the photolysis of NO₂ in a closed quartz vessel. This static chemical actinometer compares well with the chemical flow NO₂ actinometer of Forschungszentrum Jülich deployed in JCOM97 [*Kraus et al.*, 2000; *Kraus and Hofzumahaus*, 1998].

2.3.2. Forschungszentrum Jülich

[21] The $j(\text{NO}_2)$ filter radiometer of FZJ used during IPMMI was a commercial instrument manufactured by METCON. During IPMMI the filter radiometer signal was recorded by a data logging system with an integration time of 60 s. The $j(\text{NO}_2)$ values were determined by applying a constant conversion factor to the radiometer signal. The FZJ filter radiometer calibration constant applied during IPMMI was determined against a chemical flow actinometer during the JCOM97 field campaign at Forschungszentrum Jülich in June 1997 [*Kraus et al.*, 1998]. No further correction was made for either a possible temperature dependence of the

NO₂ photodissociation process or for imperfect angular and spectral response of the radiometer. This simplification leads to systematic errors in the $j(\text{NO}_2)$ filter radiometer that are discussed in more detail by *Cantrell et al.* [2003] and *Lefer et al.* [2001b]. The FZJ filter radiometer data submitted for 18 June were the raw voltages which were a factor of $1/1.5 \times 10^{-3}$ higher than the photolysis frequencies resubmitted as revised data. The conversion factor is the calibration constant of the filter radiometer. The originally submitted 10-min and 30-min averaged $j(\text{NO}_2)$ data, however, were correctly submitted for 18 June and agree with the revised 1-min data.

2.3.3. Fraunhofer-Institut für Atmosphärische Umweltforschung

[22] The filter radiometer for $j(\text{NO}_2)$ used by Fraunhofer-Institut für Atmosphärische Umweltforschung (IFU) was originally delivered by METCON and modified at IFU with a new set of optical filters (2-mm UG3, 1-mm UG5, Schott GmbH) to increase the agreement with the $j(\text{NO}_2)$ action spectra [*Volz-Thomas et al.*, 1996]. The field of view of the filter radiometer was restricted by a 14-cm-diameter artificial horizon from METCON. Calibration is based on comparison in 1996 with a factory-calibrated instrument by METCON. The instrument was used successfully in the 1997 JCOM intercomparison campaign in Jülich. Although the instrument displayed proper diurnal variations on the ground, the instrument response proved to be unstable during IPMMI and through the end of August 1998 when the sensitivity sharply dropped during the BERLIOZ campaign. This instrument behavior could be traced to a malfunctioning electronics board. Replacement of this component resulted in even lower readings for $j(\text{NO}_2)$ compared with pre-IPMMI conditions. This decline in sensitivity (on the order of 25%) over the summer of 1998 was probably due to an aging photodiode that had been in use for more than 6 years. Possible causes of this instrument failure include the facts that (1) the instrument is not heated and often cycled between $\sim 30^\circ\text{C}$ and temperatures $< 0^\circ\text{C}$ during aircraft measurements, and (2) while the instrument is decoupled from the aircraft with a flexible support, aircraft vibrations may be a source for further stress for instrument components.

2.3.4. NASA Langley Research Center

[23] The NASA Langley Research Center (NAL) filter radiometers used during IPMMI were commercial instruments manufactured by METCON. See instrument descriptions of $j(\text{NO}_2)$ filter radiometers above. During IPMMI the filter radiometers signals were recorded by a data logging system with an integration time of 60 s. The $j(\text{NO}_2)$ values were determined by applying a constant conversion factor supplied by the manufacturer to the radiometer signals. The NAL filter radiometer calibration constants applied during IPMMI were determined by METCON, by comparison, in 1997 with a factory-calibrated instrument.

2.3.5. University of Leicester

[24] The ULI filter radiometer used during IPMMI was a commercial instrument manufactured by METCON. During IPMMI the filter radiometer signal was recorded by a data logging system with an integration time of 60 s. The $j(\text{NO}_2)$ values were determined by applying a constant conversion factor supplied by the manufacturer to the radiometer signal. The ULI filter radiometer calibration constant applied dur-

Table 2. Listing of Instrumental Error Estimates

Instrument Type	IPMMI ID	Instrumental Errors, %	Other Errors, %	Overall Error, %
<i>Chemical Actinometers</i>				
Flow tube/NO detection	NCAR	7.3	5 ^a	8.8
Flow tube/NO detection	UMD	8	9 ^b	12
<i>Spectroradiometers</i>				
Double monochromator/photomultiplier (Mono/PMT)	FZJ	5	10.8 ^c	11.9
Double Mono/PMT	NCAR	5	10.8 ^c	11.9
Double Mono/PMT	NIWA	6	10.8 ^c	12.4
Single Mono diode array	MET	8–10 ^d	10.8 ^c	13.4–15
Single Mono diode array	ULI	8–10 ^d	10.8 ^c	13.4–15
<i>Filter Radiometer</i>				
MetCon jNO ₂ radiometer	FZJ	7	6.5–8.5 ^{e,f}	9.6–11
MetCon jNO ₂ radiometer	IFU	20	6.5–8.5 ^{e,f}	21.0–21.7
MetCon jNO ₂ radiometer	MET1	7	6.5–8.5 ^{e,f}	9.6–11
MetCon jNO ₂ radiometer	MET2	7	6.5–8.5 ^{e,f}	9.6–11
MetCon jNO ₂ radiometer	NAL1	7	6.5–8.5 ^{e,f}	9.6–11
MetCon jNO ₂ radiometer	NAL2	7	6.5–8.5 ^{e,f}	9.6–11
MetCon jNO ₂ radiometer	ULI	7	6.5–8.5 ^{e,f}	9.6–11

^aError associated with instrument sensitivity drift.

^bError associated with system leak.

^cError associated with NO₂ cross section (4%) and quantum yield (10%).

^dError associated with low (8%) and high (10%) solar zenith angles.

^eError associated with temperature stability and imperfect angular and spectral response.

^fTotal other error associated with clear (6.5%) and cloudy (8.5%) conditions.

ing IPMMI was determined by METCON, by comparison, in 1997 with a factory-calibrated instrument.

2.4. Instrumental Uncertainties

[25] It is important to understand the uncertainties associated with the different $j(\text{NO}_2)$ instruments when comparing the reported IPMMI results. Detailed error analysis calculations of the $j(\text{NO}_2)$ measurement error for each instrument is reported in Table 2. The overall error is a combination of the instrument error (e.g., calibration, light collection) and other errors not related to the operation of the instrument but included in the final reported $j(\text{NO}_2)$ value.

2.5. Calculations of $j(\text{NO}_2)$

[26] Model calculations of $j(\text{NO}_2)$ for IPMMI were submitted for 15 models from 13 institutions. A listing of the

participating institutions, IPMMI identification, and specific model used is shown in Table 3. Details concerning these models are given by *Cantrell et al.* [2003] and *Bais et al.* [2003]. By virtue of its photolysis at longer wavelengths (~320–410 nm), $j(\text{NO}_2)$ is nearly insensitive to overhead ozone conditions, rendering it less difficult to predict than $j(\text{O}^1D)$ and other important j values with significant spectral overlap. *Madronich and Weller* [1990] have also shown $j(\text{NO}_2)$ to be fairly robust with respect to wavelength resolution compared to other important photolysis frequencies, e.g., $j(\text{O}^1D)$, $j(\text{CH}_2\text{O})$, and $j(\text{HNO}_3)$. For wavelength resolutions of 1 nm and 10 nm, differences in $j(\text{NO}_2)$ were <1%.

[27] Past investigations of $j(\text{NO}_2)$ have shown calculations to be prone to underestimates of 20% or more when using two-stream versus multistream methods [*Ruggaber et al.*, 1993; *Olson et al.*, 1997]. Here only models employing four streams or greater have been used, except for the JHU model,

Table 3. Listing of Participating Modeling Groups, IPMMI ID, and Model Used

Modeling Group	IPMMI ID	Model
National Center for Atmospheric Research ACD	ACD	TUV 4.0
Environment Canada	AES	JMAM
British Antarctic Survey	BAS	BASRTM
Fraunhofer Institut Atmosphärische Umweltforschung	BM1	LibRadtran
Fraunhofer Institut Atmosphärische Umweltforschung	BM2	LibRadtran
Fraunhofer Institut Atmosphärische Umweltforschung	BM3	LibRadtran
Johns Hopkins University Applied Physics Laboratory	JHU	JHU/APL
Forschungszentrum Jülich	FZJ	ART
Karl-Franzens University	KFU	TUV 3.9
Royal Netherlands Meteorological Institute	KNM	DAK
Institute for Marine and Atmospheric Research	MAR	Parametric
Norwegian Institute for Air Research	NI1	LibRadtran
Norwegian Institute for Air Research	NI2	photodis
NOAA Aeronomy Laboratory	NOA	TUV 3.8
Meteorologisches Institut Universität München	UMU	STAR

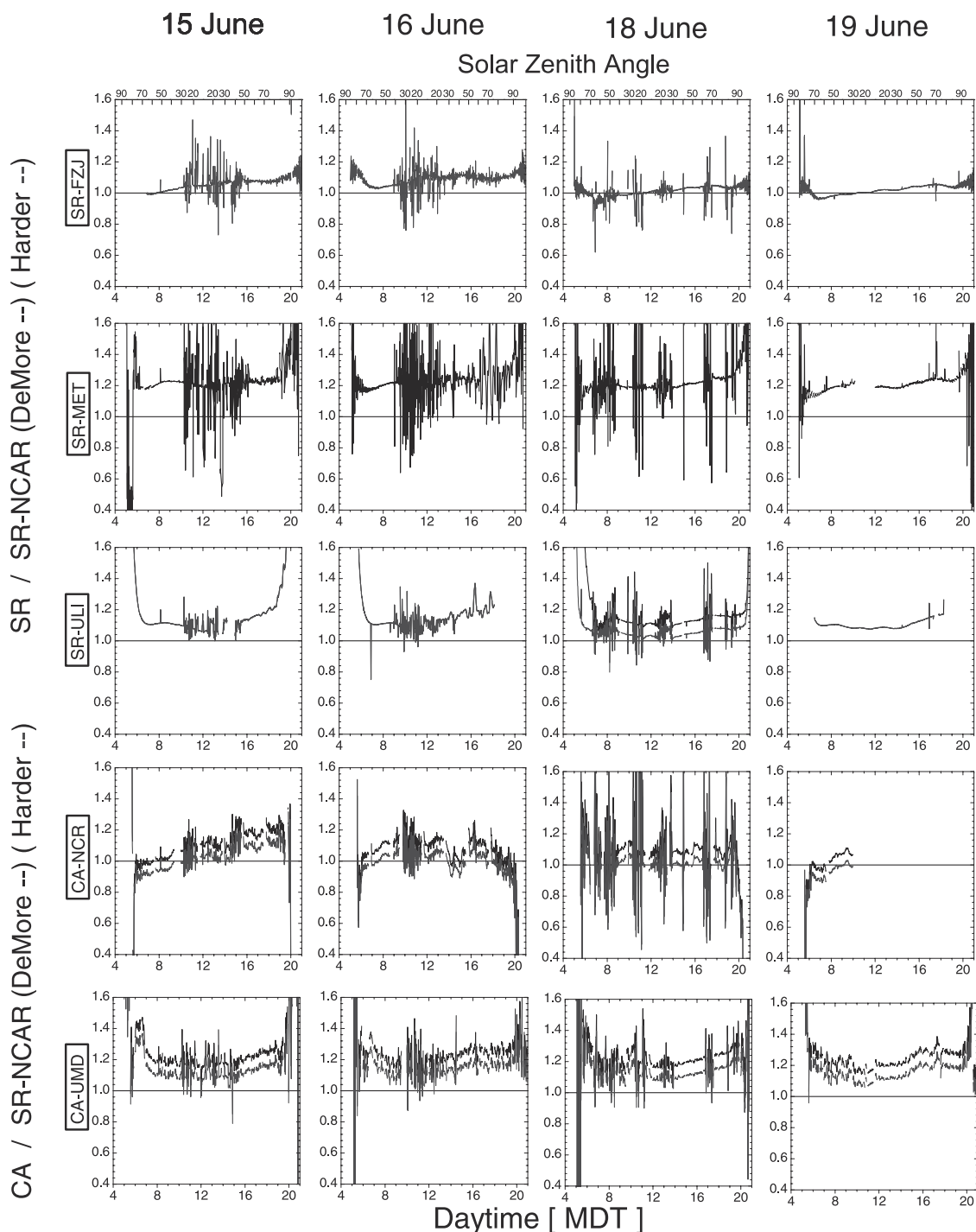


Figure 1a. Plots of the ratios of the 1-min $j(\text{NO}_2)$ spectroradiometer data for three spectroradiometers and $j(\text{NO}_2)$ data chemical actinometer for two chemical actinometers to the National Center for Atmospheric Research (NCAR) spectroradiometer $j(\text{NO}_2)$ data for 15, 16, 18, and 19 June. Solid lines are ratios using *DeMore et al.*'s [1997] NO_2 cross-section data for spectroradiometer photolysis frequency calculations, and red lines are ratios using *Harder et al.*'s [1997] NO_2 cross-section data for spectroradiometer photolysis frequency calculations. The spectroradiometer from Meteorologie Consult GmbH (SR-MET) did not submit data using *Harder et al.* [1997] cross-section data, and the ratios for the spectroradiometer from Forschungszentrum Jülich (SR-FZJ) and spectroradiometer from the University of Leicester (SR-ULI) *DeMore et al.* [1997] and *Harder et al.* [1997] data overlap except for SR-ULI on 18 June. See color version of this figure at back of this issue.

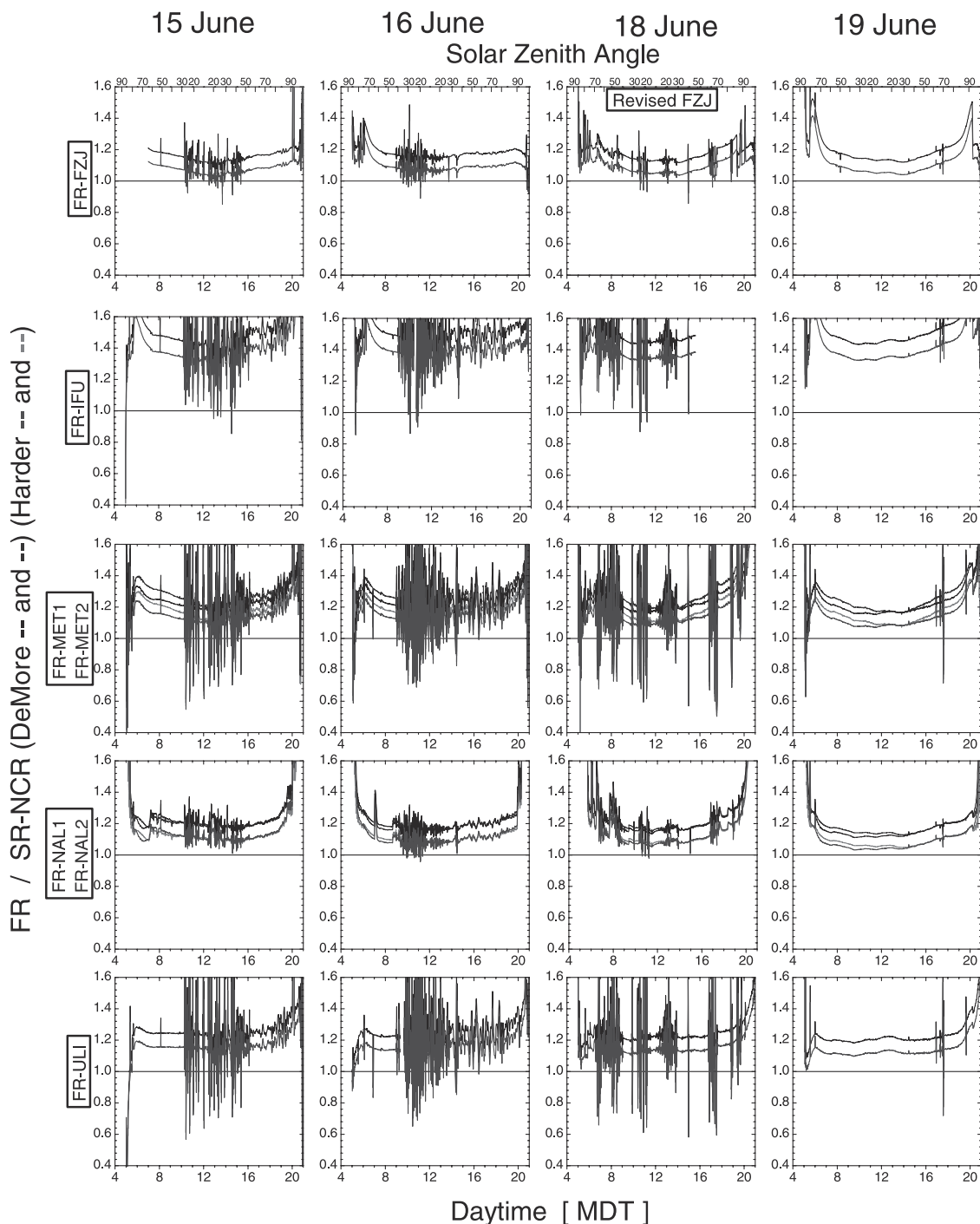


Figure 1b. Plots of the ratios of 1-min filter radiometer $j(\text{NO}_2)$ data for seven filter radiometers to the NCAR spectroradiometer $j(\text{NO}_2)$ data for 15, 16, 18, and 19 June. Black and blue lines are ratios using *DeMore et al.* [1997] NO₂ cross-section data for spectroradiometer photolysis frequency calculations, and red and orange lines are ratios using *Harder et al.* [1997] NO₂ cross-section data for spectroradiometer photolysis frequency calculations. See color version of this figure at back of this issue.

which solves the integral equation of radiative transfer and highly parameterized MAR model; therefore differences due to choice of algorithm are likely to be small.

[28] While the choice of spectral data for the absorption cross section and quantum yield is important for the accuracy of model estimates for $j(\text{NO}_2)$, this consideration

plays only a small role in any differences between models. With the exception of five models (BM1, BM2, BM3, KFA, and UMU) the spectral data for NO₂ have been taken from the Jet Propulsion Laboratory (JPL) recommendation, which has not changed in over a decade [*DeMore et al.*, 1992, 1994, 1997]. The other five models employed the

Table 4. Slopes of the Correlation Line of the Ratio of $j(\text{NO}_2)$ From Each Instrument to the $j(\text{NO}_2)$ Determined by the National Center for Atmospheric Research Spectroradiometer^a

Instrument	Correlation Line Slopes							
	<i>DeMore et al.</i> [1997], CS				<i>Harder et al.</i> [1997], CS			
	15 June 2002	16 June 2002	18 June 2002	19 June 2002	15 June 2002	16 June 2002	18 June 2002	19 June 2002
Spectroradiometer (SR) FZJ	1.044	1.060	1.013	1.016	1.044	1.061	1.014	1.017
SR MET	1.138	1.120	1.175	1.199				
SR ULI	1.052	1.061	1.105	1.046	1.053	1.061	1.031	1.047
Chemical actinometer (CA) NCAR	1.087	1.131	1.055	1.093	1.010	1.048	0.987	1.015
CA UMD	1.138	1.179	1.192	1.205	1.082	1.095	1.107	1.118
Filter radiometer (FR) FZJ	1.130	1.146	1.128	1.115	1.050	1.064	1.047	1.035
FR IFU	1.371	1.460	1.435	1.433	1.273	1.356	1.333	1.330
FR MET1	1.171	1.172	1.153	1.150	1.087	1.088	1.071	1.068
FR MET2	1.196	1.204	1.174	1.164	1.111	1.118	1.090	1.081
FR NAL1	1.191	1.151	1.137	1.113	1.106	1.069	1.056	1.034
FR NAL2	1.191	1.166	1.145	1.129	1.106	1.083	1.063	1.048
FR ULI	1.205	1.193	1.193	1.197	1.119	1.108	1.107	1.111

^aSlopes are for all 4 measurement days using both the *DeMore et al.* [1997] and *Harder et al.* [1997] NO₂ cross-section data.

cross-section data of *Schneider et al.* [1987], which is only slightly lower than the *Davidson et al.* [1988] work on which the JPL recommendation is based. For a given model calculation of actinic flux, substituting the *Schneider et al.* [1987] cross sections for the JPL recommendation should lead to reductions in $j(\text{NO}_2)$ of no more than 3%.

[29] Aerosol profiles for model inputs are the least consistent between the models participating in IPMMI. Models used everything from no aerosol (MAR) as inputs to profiles from *Elterman* [1968] (KFU, NOA) and *Shettle and Fenn* [1979] (BAS, BM1, BM2, BM3, and NIL) and profiles scaled to IPMMI conditions (ACD, AES, and JHU) (Table 3). These differences are detailed by *Bais et al.* [2003]. Differences due to aerosol assumptions are also more difficult to quantify. The photolysis of NO₂ is only weakly dependent on the temperature [*Shetter et al.*, 1988; *Roehl et al.*, 1994], so differences in temperatures used by the models should lead to differences of no more than 2%.

3. Results and Discussion

3.1. Comparison of Experimental Results

[30] The $j(\text{NO}_2)$ instruments were operated continuously for 4 days (15, 16, 18, and 19 June 1998) at the Marshall field facility near Boulder, Colorado. A detailed description of the measurement site and the atmospheric conditions can be found in the IPMMI overview paper by *Cantrell et al.* [2003]. The instruments measured the $j(\text{NO}_2)$ from downwelling radiation at ~ 5 m above the ground. The data were reported to the referee in 1-, 10-, and 30-min averages. The first 2 days (15 and 16 June) had clear conditions in the early mornings with clouds building in the afternoons. Intermittent clouds were visible throughout the entire day of 18 June, while 19 June was a quite clear day with almost no clouds. All instruments reported data for the entire 4-day period except for the NCAR chemical actinometer that experienced a failure at 1000 LT on the last day of the experiments, 19 June.

3.2. Measurement Ratios

[31] Plots of the ratios of the $j(\text{NO}_2)$ determined by each of the spectroradiometers, filter radiometers, and chemical

actinometers to the NCAR spectroradiometer data for the 4 measurement days are shown in Figures 1a and 1b. The *DeMore et al.* [1997] recommendations for the absorption cross section of NO₂ are based on the *Davidson et al.* [1988] data, but in the last 8 years other several investigators have reported cross sections that are 5–7% higher [*Merienne et al.*, 1995; *Harder et al.*, 1997]. Since the data from the spectroradiometers depend directly on the cross section used in the calculations, plots of the ratio of the final $j(\text{NO}_2)$ data determined with the various instruments to the NCAR spectroradiometer data calculated using both the *DeMore et al.* [1997] and *Harder et al.* [1997] cross sections are shown. One can see from the ratio plots that the data at small solar zenith angles from all of the instruments agree within 10–30% on all 4 measurement days, regardless of cross section used, with the exception of the data from the IFU filter radiometer. The IFU filter radiometer was found to have hardware problems detailed in the instrumentation description section above. The agreement of the filter radiometers at solar zenith angles $>70^\circ$ varies from 20 to 50%, indicating angular collection differences of the optical collectors or incorrect offset corrections. Most of the instruments show a high-frequency noise on the ratio plots for 15, 16, and 18 June. This noise is attributable to intermittent clouds and the differing time response of the various instruments and is not observed on 19 June, the nearly cloud-free day. In order to quantitatively assess the agreement, correlations of the 1-min instrument data with the NCAR spectroradiometer data for 15, 16, 18, and 19 June were performed and the slopes of the correlation line tabulated in Table 4. The correlations were done for spectroradiometer data calculated from both the *DeMore et al.* [1997] and *Harder et al.* [1997] cross-section data. All of the instruments demonstrated very high correlation factors (R^2) of 0.992 or better with 9 of the 12 instruments with R^2 values 0.997 or better, regardless of cross section used. Offsets of the correlations generally were small, with the largest offset equivalent to a bias of $<3\%$ for noontime $j(\text{NO}_2)$. The slopes of the correlations highlight the large discrepancy in the IFU filter radiometer data, with 27–46% higher photolysis frequencies. All of the filter radiometers except the FZJ and IFU radiometers used the manufacturer's calibration data.

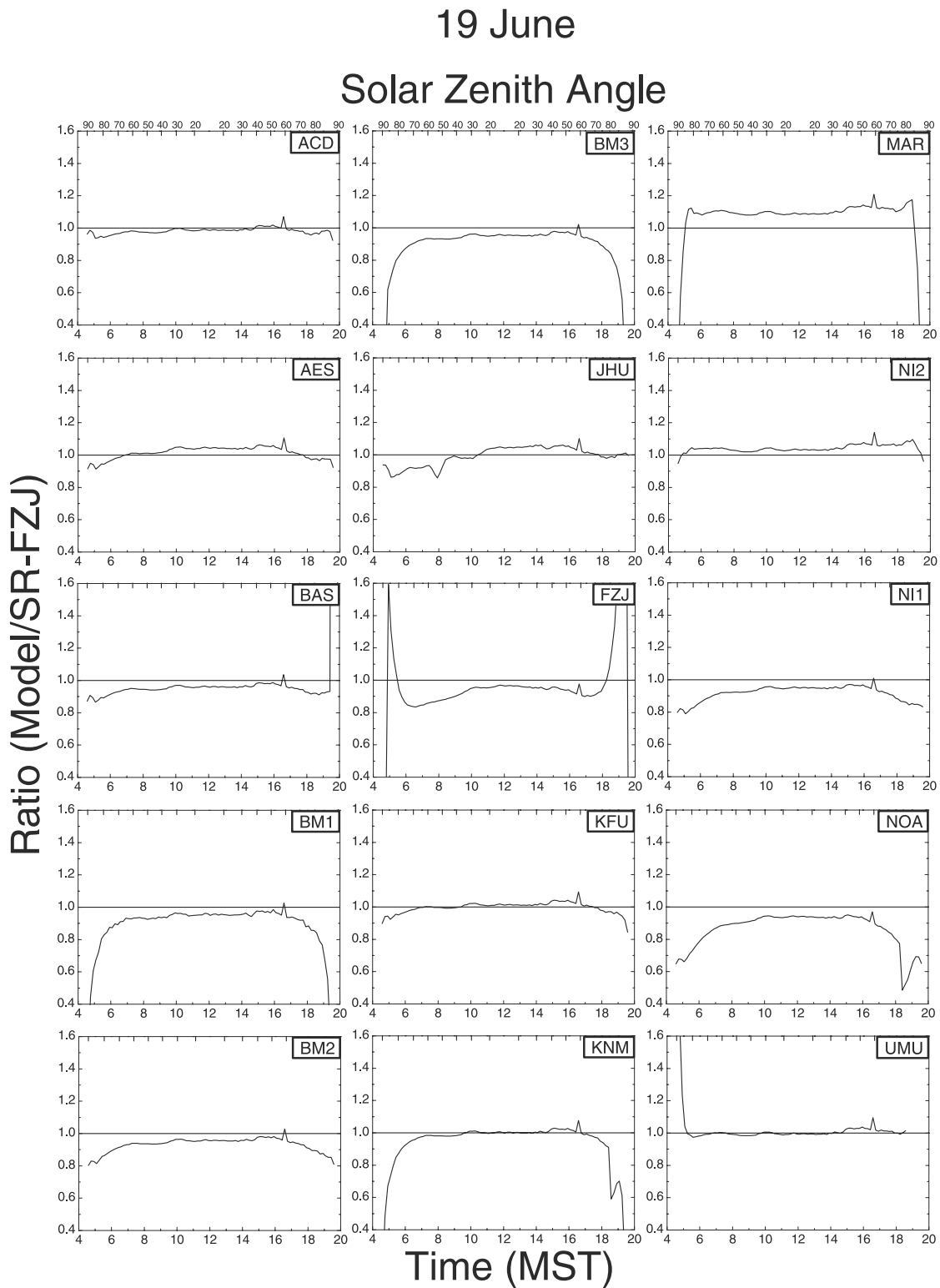


Figure 2. Plots of the ratios of 10-min model calculated $j(\text{NO}_2)$ data to the 10-min Forschungszentrum Jülich spectroradiometer $j(\text{NO}_2)$ data using *DeMore et al.* [1997] cross-section data for 19 June for 15 models.

[32] Absent from the comparisons are the data from the NIWA irradiance spectroradiometer. The comparison of the “pseudo”-actinic fluxes and photolysis frequencies calculated from the NIWA instrument data with the FZJ and NCAR actinic flux spectroradiometer data are described by *McKenzie et al.* [2002].

3.3. Comparison of Experimental Data With Model Calculations

[33] Fifteen sets of calculated $j(\text{NO}_2)$ using either the *DeMore et al.* [1997] or the *Schneider et al.* [1987] NO₂ cross-section data were submitted during IPMMI. After model comparisons were circulated to the IPMMI participants, four groups discovered errors in their original calculations and resubmitted revised data. These groups and the reasons for resubmitting are discussed by *Bais et al.* [2003]. The revised data from all groups are used for these comparisons. Diurnal plots of the ratio of model calculations to the FZJ spectroradiometer data for 19 June 1998 using the *DeMore et al.* [1997] data are shown in Figure 2. Since both the models and the spectroradiometers use cross-section data in calculating the photolysis frequencies, no comparisons with the larger cross-section data of *Harder et al.* [1997] with the spectroradiometer data are needed. The models agree with the spectroradiometer measurements to the 10% level during the central part of the day when the solar zenith angles are $<70^\circ$. Although not shown, model agreement with the chemical actinometers is improved by the use of the higher cross-section data of *Harder et al.* [1997]. At larger solar zenith angles the ratio of calculated value to measured value deviates significantly from unity for the BM1, BM3, FZJ, NOA, and KNM models. The MAR, BAS, and UMU models also differ significantly from the FZJ spectroradiometer data at the largest zenith angles, though the big discrepancies start at larger angles than in the other models mentioned as having discrepancies. Excellent agreement (within a few percent) throughout the diurnal cycle is exhibited by the ACD, AES, JHU, NI2, and UMU models (Table 3). In order to assess the quantitative agreement of the measurement-model comparison, correlations of the model calculation with the FZJ spectroradiometer data were performed and the slopes, offsets, and R^2 values of the correlation plots tabulated in Table 5. Comparison of experimental data with model calculations is as follows: Five models (BM1, BM3, FZJ, NOA, and KNM) do not behave well for solar zenith angles of 70° or larger (Table 3). For the BM1, BM3, and KNM models this behavior is caused by the use of plane-parallel geometry instead of pseudospherical geometry.

[34] Of the 15 models, 11 have slopes that differ from unity by $<5\%$, and 8 of these differ by $<3\%$. The five models that used the NO₂ cross sections of *Schneider et al.* [1987] all have slopes lower than unity, but for four of the five, this difference is less than the $\sim 3\%$ reduction expected relative to using the *DeMore et al.* [1997] recommendations.

4. Conclusions

[35] Consistent results for the NO₂ photolysis frequencies were obtained using measurements of the actinometers, filter radiometers, and spectroradiometers, with better agreement when the higher NO₂ cross-section data of *Harder et al.*

Table 5. Slopes, Intercepts, and R^2 Values for the Correlation Line of the Model Data to the $j(\text{NO}_2)$ Determined by the Forschungszentrum Jülich Spectroradiometer

Model	Slope	Offset, s ⁻¹	R^2
ACD	0.994	-4.0×10^{-5}	0.999
AES	1.055	-1.4×10^{-4}	0.998
BAS	0.965	-4.0×10^{-5}	0.998
BM1	0.982	-2.2×10^{-4}	0.998
BM2	0.971	-1.2×10^{-4}	0.999
BM3	0.982	-2.2×10^{-4}	0.999
JHU	1.044	-2.0×10^{-4}	0.998
FZJ	0.926	$+5.8 \times 10^{-5}$	0.998
KFU	1.024	-7.6×10^{-5}	0.999
KNM	1.035	-2.5×10^{-4}	0.998
MAR	1.100	$+1.7 \times 10^{-5}$	0.998
NI1	0.968	-1.7×10^{-4}	0.998
NI2	1.032	$+5.6 \times 10^{-5}$	0.999
NOA	0.980	-3.9×10^{-4}	0.995
UMU	0.989	$+8.0 \times 10^{-5}$	0.998

[1997] are used in the spectroradiometer calculations. The data for the 4 days of measurements from the UMD chemical actinometer are from 8.2 to 11.8% higher when compared with the NCAR spectroradiometer using the *Harder et al.* [1997] data and 13.8 to 20.5% higher using the *DeMore et al.* [1997] data, while the NCAR chemical actinometer is from -1.3 to 4.8% different and 8.7 to 13.1% higher in the same comparisons. The actinometers and spectroradiometers (using the *Harder et al.* [1997] cross section) were in excellent agreement throughout the campaign, to well within the uncertainties of the individual instruments, with the NCAR and FZJ spectroradiometers and the NCAR actinometer differing by $<2\%$ on average under clear-sky conditions. Since spectroradiometers are calibrated using an irradiance standard and the actinometers are calibrated using gas phase standards, either the uncertainty in the molecular data used in calculating $j(\text{NO}_2)$ and the uncertainties associated with the actinometer determination have a canceling effect or the uncertainties in both may be overestimated. A recent reevaluation of the cross section and quantum yield data by the International Union of Pure and Applied Chemistry (IUPAC) recommends the higher cross-section data in close accord with the *Merienne et al.* [1995] data and revised quantum yield data from *Troe* [2000]. Use of the recommended IUPAC data gives excellent agreement between the spectroradiometers and chemical actinometers in both JCOM97 and the IPMMI studies. Filter radiometer measurements appear to be of lower accuracy and generally suggest from 4 to 10% higher values than the spectroradiometer data calculated from the higher cross sections from *Harder et al.* [1997] and from 11 to 20% using the recommended data from *DeMore et al.* [1997], with larger discrepancies at large solar zenith angles. Since the filter radiometer calibrations are tied to chemical actinometers, better agreement would be expected with the data using the higher cross sections based on the spectroradiometer-chemical actinometer level of agreement. The model $j(\text{NO}_2)$ results from most modeling groups show reasonably good agreement with measurements (within 5%) for the clear-sky conditions at small to moderate solar zenith angles but with deviations growing significantly in some cases at solar zenith angles of 70° or larger. A few models gave results with significant deviations ($\sim 10\%$) from the measurements at most of the solar zenith angle values. Of

course, models cannot be expected to agree as well for less than ideal conditions, especially when critical input parameters are poorly known (e.g., optical depths of clouds, aerosols, and ozone columns) or when the atmospheric optical complexity (e.g., from broken cloud fields) cannot be well represented in the models.

[36] It can be concluded that the calculation of clear-sky $j(\text{NO}_2)$ values can yield accurate results at small to moderate solar zenith angles for most of the radiative transfer models employed by atmospheric scientists today, but the accuracy depends heavily on the accuracy of the molecular parameters used in these calculations. Instrumental measurements of $j(\text{NO}_2)$ agree within the uncertainty of the individual instruments and indicate that the uncertainty in the instruments or in the molecular parameters may be overestimated. This agreement improves somewhat with the use of the higher NO₂ cross-section data reported by Harder et al. [1997].

[37] Recently, B. L. Lefer et al. (Impact of clouds and aerosols on photolysis frequencies and photochemistry during TRACE-P: 1. Analysis using radiative transfer and photochemical box models, submitted to *Journal of Geophysical Research*, 2002) have examined the sensitivity of photochemical box models to photolysis frequency inputs. This study determined that O₃ production and loss rates change linearly with errors in the photolysis frequency inputs, with the O₃ production rate changing with a steeper slope than the O₃ loss rate. The net O₃ tendency has a positive linear response (with a slope close to 1) to errors in photolysis frequencies; thus a +10% error in measured j values would result in approximately a 10% overestimate of the instantaneous net O₃ tendency.

[38] **Acknowledgment.** The National Center for Atmospheric Research is operated by the University Corporation for Atmospheric Research under the sponsorship of the National Science Foundation.

References

- Bahe, F. C., The frequency of NO₂ photolysis at ground level, as recorded by continuous actinometer, *Atmos. Environ.*, **14**, 711–718, 1980.
- Bais, A. F., et al., International photolysis frequency measurement and modeling intercomparison: Spectral actinic solar flux measurements and modeling, *J. Geophys. Res.*, **108**(D16), 8543, doi:10.1029/2002JD002891, in press, 2003.
- Brauers, T., and A. Hofzumahaus, Latitudinal variation of measured NO₂ photolysis frequencies over the Atlantic Ocean between 50°N and 30°S, *J. Atmos. Chem.*, **15**, 269–282, 1992.
- Brauers, T., H. P. Dorn, H. Koch, A. B. Kraus, and C. Plass-Dulmer, Meteorological aspects, ozone, and solar radiation measurements during POPCORN 1994, *J. Atmos. Chem.*, **31**, 33–52, 1998.
- Burkert, J., M. D. Andres-Hernandez, D. Stobener, J. P. Burrows, M. Weissenmayer, and A. Kraus, Peroxy radical and related trace gas measurements in the boundary layer above the Atlantic Ocean, *J. Geophys. Res.*, **106**, 5457–5477, 2001.
- Cantrell, C., J. Calvert, A. F. Bais, R. E. Shetter, B. Lefer, and G. Edwards, Overview and conclusions of the International Photolysis Frequency Measurement and Modeling Intercomparison (IPMMI) study, *J. Geophys. Res.*, **108**(D16), 8542, doi:10.1029/2002JD002962, in press, 2003.
- Davidson, J. A., C. A. Cantrell, A. H. McDaniel, R. E. Shetter, S. Madronich, and J. G. Calvert, Visible-ultraviolet absorption cross sections for NO₂ as a function of temperature, *J. Geophys. Res.*, **93**, 7105–7112, 1988.
- DeMore, W. B., M. J. Molina, S. P. Sander, D. M. Golden, C. E. Kolb, R. F. Hampson, M. J. Kurylo, C. J. Howard, and A. R. Ravishankara, Chemical kinetics and photochemical data for use in stratospheric modeling, *JPL Publ.*, **92-20**, 111–112, 1992.
- DeMore, W. B., M. J. Molina, S. P. Sander, D. M. Golden, C. E. Kolb, R. F. Hampson, M. J. Kurylo, C. J. Howard, and A. R. Ravishankara, Chemical kinetics and photochemical data for use in stratospheric modeling, *JPL Publ.*, **94-26**, 119–121, 1994.
- DeMore, W. B., S. P. Sander, D. M. Golden, R. F. Hampson, M. J. Kurylo, C. J. Howard, A. R. Ravishankara, C. E. Kolb, and M. J. Molina, Chemical kinetics and photochemical data for use in stratospheric modeling, *JPL Publ.*, **97-4**, 155–157, 1997.
- Dickerson, R. R., D. H. Stedman, and A. C. Delany, Direct measurements of ozone and nitrogen dioxide photolysis rates in the troposphere, *J. Geophys. Res.*, **87**, 4933–4946, 1982.
- Dickerson, R. R., S. Kondragunta, G. Stenchikov, K. L. Civerolo, B. G. Doddridge, and B. Holben, The impact of aerosols on solar ultraviolet radiation and photochemical smog, *Science*, **278**(5339), 827–830, 1997.
- Early, E. A., E. A. Thompson, and P. Disterhoft, Field calibration unit for ultraviolet spectroradiometers, *Appl. Opt.*, **37**(28), 6664–6670, 1998.
- Edwards, G. D., and P. S. Monks, Performance of a single monochromator diode array spectroradiometer for the determination of actinic flux and atmospheric photolysis frequencies, *J. Geophys. Res.*, **108**(D16), 8546, doi:10.1029/2002JD002844, in press, 2003.
- Elterman, L., UV, visible, and IR attenuation for altitudes to 50 km, *Rep. AFCRL-68-0153*, Air Force Cambridge Res. Lab., Cambridge, Mass., 1968.
- Harder, J. W., J. W. Brault, P. V. Johnston, and G. H. Mount, Temperature dependent NO₂ cross sections at high spectral resolution, *J. Geophys. Res.*, **102**, 3861–3879, 1997.
- Harvey, R. B., D. H. Stedman, and W. Chamedies, Determination of the absolute rate of solar photolysis of NO₂, *J. Air Pollut. Control Assoc.*, **27**, 663–666, 1977.
- Hofzumahaus, A., A. Kraus, and M. Müller, Solar actinic flux spectroradiometry: A technique for measuring photolysis frequencies in the atmosphere, *Appl. Opt.*, **38**(21), 4443–4460, 1999.
- Jackson, J. O., D. H. Stedman, R. G. Smith, L. H. Hecker, and P. O. Warner, Direct NO₂ photolysis rate monitor, *Rev. Sci. Instrum.*, **46**, 376–378, 1975.
- Junkermann, W., U. Platt, and A. Volz-Thomas, A photoelectric detector for the measurement of photolysis frequencies of ozone and other atmospheric molecules, *J. Atmos. Chem.*, **8**, 203–227, 1989.
- Kelley, P., R. R. Dickerson, W. T. Luke, and G. L. Kok, Rate of NO₂ photolysis from the surface to 7.6-km altitude in clear sky and clouds, *Geophys. Res. Lett.*, **22**, 2621–2624, 1995.
- Kraus, A., and A. Hofzumahaus, Field measurements of atmospheric photolysis frequencies for O₃, NO₂, HCHO, CH₃CHO, H₂O₂, and HONO by UV spectroradiometry, *J. Atmos. Chem.*, **31**, 161–180, 1998.
- Kraus, A., T. Brauers, D. Brüning, A. Hofzumahaus, F. Rohrer, N. Houben, H.-W. Pätz, and A. Volz-Thomas, Ergebnisse des NO₂: Photolysefrequenz meßvergleichs JCOM97, *Ber. Jül-3578*, 45 pp., Forschungszentrum Jülich, Jülich, Germany, 1998.
- Kraus, A., F. Rohrer, and A. Hofzumahaus, Intercomparison of NO₂ photolysis frequency measurements by actinic flux spectroradiometry and chemical actinometry during JCOM97, *Geophys. Res. Lett.*, **27**, 1115–1118, 2000.
- Lantz, K. O., R. E. Shetter, C. A. Cantrell, S. J. Flocke, J. G. Calvert, and S. Madronich, Theoretical, actinometric, and radiometric determinations of the photolysis rate coefficient of NO₂ during the Mauna Loa Observatory Photochemistry Experiment 2, *J. Geophys. Res.*, **101**, 14,613–14,629, 1996.
- Lefer, B. L., S. R. Hall, L. Cinquini, R. E. Shetter, J. D. Barrick, J. H. Crawford, J. D. Barrick, and J. H. Crawford, Comparison of airborne NO₂ photolysis frequency measurements during PEM-Tropics B, *J. Geophys. Res.*, **106**, 32,645–32,656, 2001a.
- Lefer, B. L., S. R. Hall, L. Cinquini, and R. E. Shetter, Photolysis Frequency Measurements at the South Pole during ISCAT-98, *Geophys. Res. Lett.*, **28**, 3637–3640, 2001b.
- Madronich, S., Photodissociation in the atmosphere: 1. Actinic flux and the effects of ground reflections and clouds, *J. Geophys. Res.*, **92**, 9740–9752, 1987.
- Madronich, S., and G. Weller, Numerical integration errors in calculated tropospheric photodissociation rate coefficients, *J. Atmos. Chem.*, **10**, 289–300, 1990.
- Madronich, S., D. R. Hastie, B. A. Ridley, and H. I. Schiff, Measurement of the photodissociation coefficient of NO₂ in the atmosphere, I, Method and surface measurements, *J. Atmos. Chem.*, **2**, 3–25, 1984.
- Madronich, S., D. R. Hastie, B. A. Ridley, and H. I. Schiff, Measurement of the photodissociation coefficient of NO₂ in the atmosphere, II, Stratospheric measurements, *J. Atmos. Chem.*, **3**, 233–245, 1985.
- McKenzie, R. L., P. V. Johnson, M. Kotkamp, A. Bittar, and J. D. Hamlin, Solar ultraviolet spectroradiometry in New Zealand: Instrumentation and sample results from 1990, *Appl. Opt.*, **31**, 6501–6509, 1992.
- McKenzie, R. L., P. Johnston, A. Hofzumahaus, A. Kraus, S. Madronich, C. Cantrell, J. Calvert, and R. Shetter, Relationship between photolysis frequencies derived from spectroscopic measurements of actinic fluxes and irradiances during the IPMMI campaign, *J. Geophys. Res.*, **107**(D5), 4042, doi:10.1029/2001JD000601, 2002.
- Merienne, M. F., A. Jenouvrier, and B. Coquart, The NO₂ absorption spectrum: 1. Absorption cross sections at ambient temperature in the 300–500-nm region, *J. Atmos. Chem.*, **20**, 281–297, 1995.

- Olson, J., et al., Results from the Intergovernmental Panel on Climatic Change Photochemical Model Intercomparison (PhotoComp), *J. Geophys. Res.*, *102*, 5979–5991, 1997.
- Parrish, D. D., P. C. Murphy, D. L. Albritton, and F. C. Fehsenfeld, The measurement of the photodissociation rate of NO₂ in the atmosphere, *Atmos. Environ.*, *17*, 1365–1379, 1983.
- Pätz, H.-W., et al., Measurements of trace gases and photolysis frequencies during SLOPE96 and a coarse estimate of the local OH concentration from HNO₃ formation, *J. Geophys. Res.*, *105*, 1563–1583, 2000.
- Platt, U., et al., Free radicals and fast photochemistry during BERLIOZ, *J. Atmos. Chem.*, *42*, 359–394, 2002.
- Rhoads, K. P., P. Kelley, R. R. Dickerson, T. Carsey, M. Farmer, S. J. Oltmans, D. Savoie, and J. M. Prospero, The composition of the troposphere over the Indian Ocean during the monsoonal transition, *J. Geophys. Res.*, *102*, 18,981–18,995, 1997.
- Ridley, B. A., and L. C. Howlett, An instrument for nitric oxide measurements in the stratosphere, *Rev. Sci. Instrum.*, *45*, 742–746, 1974.
- Roehl, C., J. J. Orlando, G. S. Tyndall, R. E. Shetter, G. J. Vazquez, C. A. Cantrell, and J. G. Calvert, Temperature dependence of the quantum yields for the photolysis of NO₂ near the dissociation limit, *J. Chem. Phys.*, *98*, 3739–3743, 1994.
- Ruggaber, A., R. Forkel, and R. Dlugi, Spectral actinic flux and its ratio to spectral irradiance by radiation transfer calculations, *J. Geophys. Res.*, *98*, 1151–1162, 1993.
- Schneider, W., G. K. Moortgat, G. S. Tyndall, and J. P. Burrows, Absorption cross-sections of NO₂ in the UV and visible region (200–700 nm) at 298 K, *Photochem. Photobiol.*, *40*, 195–217, 1987.
- Schultz, M., N. Houben, D. Mihelcic, H.-W. Pätz, and A. Volz-Thomas, Ein chemisches Aktinometer zur Kalibrierung photoelektrischer Detektoren zur Messung von \dot{J} NO₂, *Ber. Jüil-3135*, Forschungszentrums Jülich, Jülich, Germany, 1995.
- Shetter, R. E., and M. Müller, Photolysis frequency measurements using actinic flux spectroradiometry during the PEM-Tropics mission: Instrumentation description and some results, *J. Geophys. Res.*, *104*, 5647–5661, 1999.
- Shetter, R. E., J. A. Davidson, C. A. Cantrell, N. J. Burzynski Jr., and J. G. Calvert, Temperature dependence of the atmospheric photolysis rate coefficient for NO₂, *J. Geophys. Res.*, *93*, 7113–7118, 1988.
- Shetter, R. E., A. H. McDaniel, C. A. Cantrell, S. Madronich, and J. G. Calvert, Actinometer and Eppley radiometer measurements of the NO₂ photolysis rate coefficient during the Mauna Loa Observatory Photochemistry Experiment, *J. Geophys. Res.*, *97*, 10,349–10,359, 1992.
- Shetter, R. E., L. Cinquini, B. L. Lefer, S. R. Hall, and S. Madronich, Comparison of airborne measured and calculated spectral actinic flux and derived photolysis frequencies during the PEM Tropics B mission, *J. Geophys. Res.*, *108*(D2), 8234, doi:10.1029/2001JD001320, 2003.
- Shettle, E. P., and R. W. Fenn, Models for the aerosols of the lower atmosphere and effects of humidity variations on their optical properties, *Environ. Pap. No. 676*, Air Force Geophys. Lab., Boston, Mass., 1979.
- Troe, J., Are primary quantum yields of NO₂ photolysis at $\lambda \leq 398$ nm smaller than unity?, *Int. J. Res. in Phys. Chem. and Chem. Phys.*, *5*, 573–581, 2000.
- Volz-Thomas, A., A. Lerner, H.-W. Pätz, M. Schultz, D. S. McKenna, R. Schmitt, S. Madronich, and E. P. Röth, Airborne Measurements of the Photolysis Frequency of NO₂, *J. Geophys. Res.*, *101*, 18,613–18,627, 1996.
- A. Bais, Laboratory of Atmospheric Physics, Aristotle University of Thessaloniki, GR-54006 Thessaloniki, Greece. (abais@auth.gr)
- J. D. Barrick and J. H. Crawford, NASA Langley Research Center, Hampton, VA 23681, USA. (j.h.crawford@larc.nasa.gov)
- J. G. Calvert, C. A. Cantrell, S. R. Hall, B. L. Lefer, S. Madronich, G. Pfister, and R. E. Shetter, Atmospheric Chemistry Division, National Center for Atmospheric Research, Boulder, CO 80303, USA. (calvert@acd.ucar.edu; cantrell@ncar.ucar.edu; halls@ucar.edu; sasha@acd.ucar.edu; pfister@ucar.edu)
- R. R. Dickerson, Department of Meteorology, University of Maryland, College Park, MD 20742, USA. (russ@atmos.umd.edu)
- G. D. Edwards and P. S. Monks, University of Leicester, Leicester LE1 7RH, UK. (p.s.monks@le.ac.uk)
- G. J. Frost, Cooperative Institute for Research in Environmental Sciences, University of Colorado, Boulder, CO 80303, USA. (gfrost@al.noaa.gov)
- B. Gardiner, British Antarctic Survey, Cambridge CB30ET, UK. (brian.gardiner@bas.ac.uk)
- E. Griffioen, Meteorological Service of Canada, Toronto, Ontario, Canada M3H 5T4. (erik@nimbus.yorku.ca)
- A. Hofzumahaus, A. Kraus, and M. Müller, Institut fuer Chemie und Dynamik der Geosphäre Institut II: Troposphäre, Forschungszentrum Jülich, D-52425 Jülich, Germany. (R.B.A.Koelemeijer@sron.nl)
- P. Johnston and R. McKenzie, National Institute of Water and Atmospheric Research, 50061 Lauder, New Zealand. (paul.c.johnston@asu.edu; r.mckenzie@niwa.co.nz)
- W. Junkermann and T. Martin, Institut fuer Meteorologie und Klimaforschung, Forschungszentrum Karlsruhe, D-82467 Garmisch-Partenkirchen, Germany. (junkermann@ifu.fhg.de; timothy.martin@gmx.de; bernhard.mayer@dlr.de)
- P. Koepke, A. Ruggaber, and H. Schwander, Meteorologisches Institut, Universität München, D-80333 Munich, Germany. (ggp@bimsg5.kfunigraz.ac.at; ruggaber@lrz.uni-muenchen.de)
- M. Krol, Institute for Marine and Atmospheric Research, NL-3508TA Utrecht, Netherlands. (M.Krol@phys.uu.nl)
- A. Kylling, Norwegian Institute for Air Research, N-2027 Kjeller, Norway. (arve.kylling@nilu.no)
- S. A. Lloyd, Applied Physics Laboratory, Johns Hopkins University, Laurel, MD 20723-6099, USA. (Steven.Lloyd@jhuapl.edu)
- B. Mayer, Institut fuer Physik der Atmosphäre, Deutsches Zentrum fuer Luft und Raumfahrt, D-82234 Wessling, Germany.
- E. P. Röth, Institut fuer Chemie und Dynamik der Geosphäre Institut I: Stratosphäre, Forschungszentrum Juelich, D-52425 Juelich, Germany. (ggp@bimsg5.kfunigraz.ac.at)
- R. Schmitt, Meteorologie Consult GmbH, Auf der Platt 47, D-61479 Glashütten, Germany.
- W. H. Swartz, Applied Physics Laboratory, John Hopkins University, Laurel, Maryland, USA. (bill.swartz@jhuapl.edu)
- M. van Weele, Royal Netherlands Meteorological Institute, NL-3730AE, DeBilt, Netherlands. (weelevm@knmi.nl)

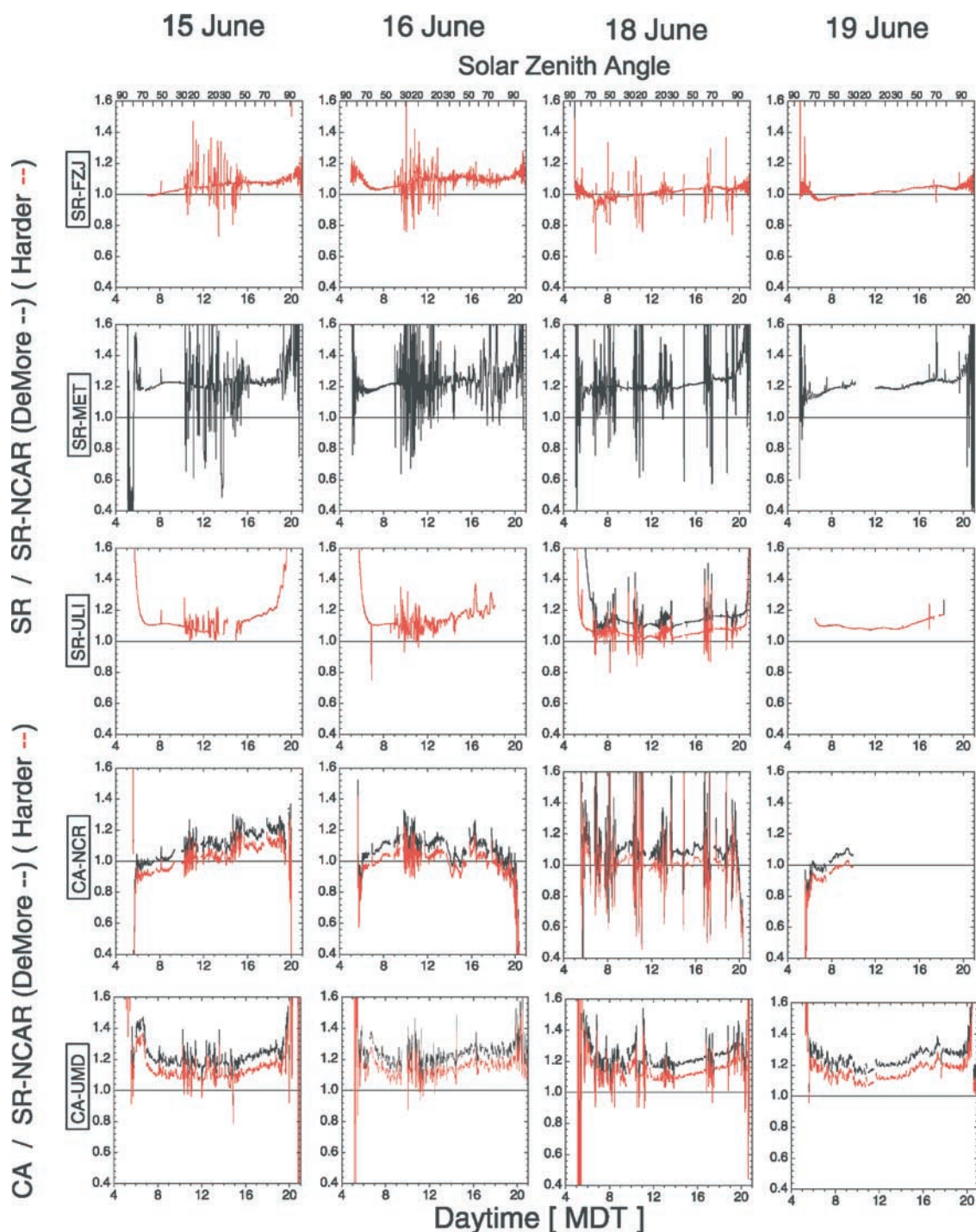


Figure 1a. Plots of the ratios of the 1-min $j(\text{NO}_2)$ spectroradiometer data for three spectroradiometers and $j(\text{NO}_2)$ data chemical actinometer for two chemical actinometers to the National Center for Atmospheric Research (NCAR) spectroradiometer $j(\text{NO}_2)$ data for 15, 16, 18, and 19 June. Solid lines are ratios using *DeMore et al.*'s [1997] NO_2 cross-section data for spectroradiometer photolysis frequency calculations, and red lines are ratios using *Harder et al.*'s [1997] NO_2 cross-section data for spectroradiometer photolysis frequency calculations. The spectroradiometer from Meteorologie Consult GmbH (SR-MET) did not submit data using *Harder et al.* [1997] cross-section data, and the ratios for the spectroradiometer from Forschungszentrum Jülich (SR-FZJ) and spectroradiometer from the University of Leicester (SR-ULI) *DeMore et al.* [1997] and *Harder et al.* [1997] data overlap except for SR-ULI on 18 June.

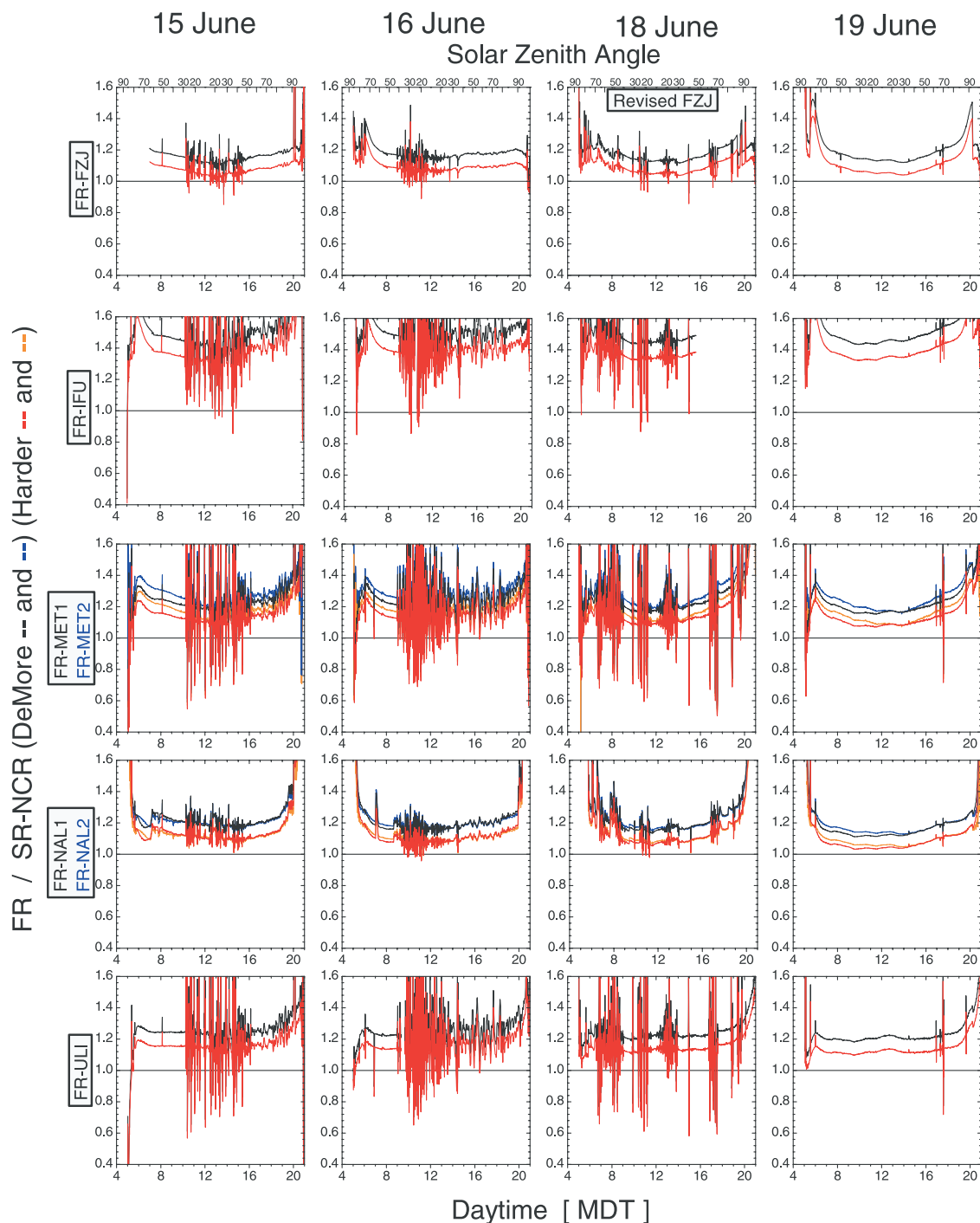


Figure 1b. Plots of the ratios of 1-min filter radiometer $j(\text{NO}_2)$ data for seven filter radiometers to the NCAR spectroradiometer $j(\text{NO}_2)$ data for 15, 16, 18, and 19 June. Black and blue lines are ratios using *DeMore et al.* [1997] NO₂ cross-section data for spectroradiometer photolysis frequency calculations, and red and orange lines are ratios using *Harder et al.* [1997] NO₂ cross-section data for spectroradiometer photolysis frequency calculations.